JACS
JOURNAL OF THE AMERICAN CHEMICAL SOCIETY
pubs.acs.org/JACS
Article

Antibody–Invertase Fusion Protein Enables Quantitative Detection of SARS-CoV-2 Antibodies Using Widely Available Glucometers

Elissa K. Leonard,◆ Miguel Aller Pellitero,◆ Boris Juelg, Jamie B. Spangler,* and Netzahualcóyotl Arroyo-Currás*

Cite This: https://doi.org/10.1021/jacs.2c02537
Read Online
ACCESS | Metrics & More | Article Recommendations | Supporting Information

ABSTRACT: Rapid diagnostics that can accurately inform patients of disease risk and protection are critical to mitigating the spread of the current COVID-19 pandemic and future infectious disease outbreaks. To be effective, such diagnostics must rely on simple, cost-effective, and widely available equipment and should be compatible with existing telehealth infrastructure to facilitate data access and remote care. Commercial glucometers are an established detection technology that can overcome the cost, time, and trained personnel requirements of current benchtop-based antibody serology assays when paired with reporter molecules that catalyze glucose conversion. To this end, we developed an enzymatic reporter that, when bound to disease-specific patient antibodies, produces glucose in proportion to the level of antibodies present in the patient sample. Although a straightforward concept, the coupling of enzymatic reporters to secondary antibodies or antigens often results in low yields, indeterminant stoichiometry, reduced target binding, and poor catalytic efficiency. Our enzymatic reporter is a novel fusion protein that comprises an antihuman immunoglobulin G (IgG) antibody genetically fused to two invertase molecules. The resulting fusion protein retains the binding affinity and catalytic activity of the constituent proteins and serves as an accurate reporter for immunoassays. Using this fusion, we demonstrate quantitative glucometer-based measurement of anti-SARS-CoV-2 spike protein antibodies in blinded clinical sample training sets. Our results demonstrate the ability to detect SARS-CoV-2-specific IgGs in patient serum with precise agreement to benchmark commercial immunoassays. Because our fusion protein binds all human IgG isotypes, it represents a versatile tool for detection of disease-specific antibodies in a broad range of biomedical applications.

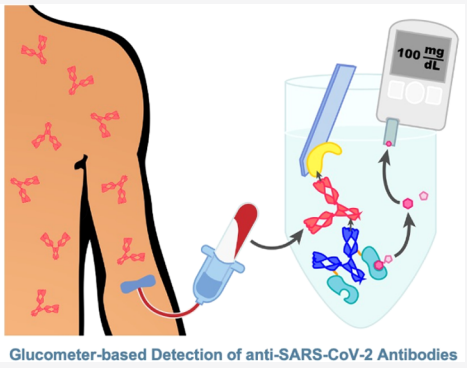

INTRODUCTION

The coronavirus disease of 2019 (COVID-19) pandemic has highlighted the importance of point-of-care, rapid diagnostic assessments that can immediately inform patients of disease risk to guide behavior and prevent disease spread.[1,2] While vaccination and prior infection provide some protection against symptomatic reinfection with the causative virus, severe acute respiratory syndrome coronavirus 2 (SARS-CoV-2), the emergence of new variants and waning of immunity have rendered many susceptible to symptomatic disease. It is still unclear what variables contribute to the longevity, or the lack thereof, of immune protection, and the current data suggests that the factors may be highly individualized.[3−5] Nonetheless, a person's level of SARS-CoV-2-specific antibodies is correlated with protection against symptomatic disease[3,4,6,7] and can therefore serve as an indicator of immune protection. Tests that measure levels of SARS-CoV-2-specific antibodies are not widely available to the general public, as the existing assays require highly skilled technicians and specialized equipment, and the vast majority of these assays must be performed in specially certified labs.[8−10] These obstacles severely limit the use of pathogen-specific antibody detection tests and thus impede characterization of immunity at the population scale, which is essential for making informed policy decisions concerning public safety measures and booster vaccinations.

The development of a rapid point-of-care diagnostic for serum antibody quantification that is broadly deployable, standardized, and does not require specialized technical skills would provide the reliable, population-wide data required to deepen epidemiological understanding of pandemics such as COVID-19.[11] This knowledge would establish the level and durability of vaccine protection, which will be vital in constructing public health and vaccination recommendations in the near- and long-term. Furthermore, a test that can be used broadly and with consistent, accurate results would provide information about key differences in infection- versus

Received: March 7, 2022

https://doi.org/10.1021/jacs.2c02537
J. Am. Chem. Soc. XXXX, XXX, XXX−XXX

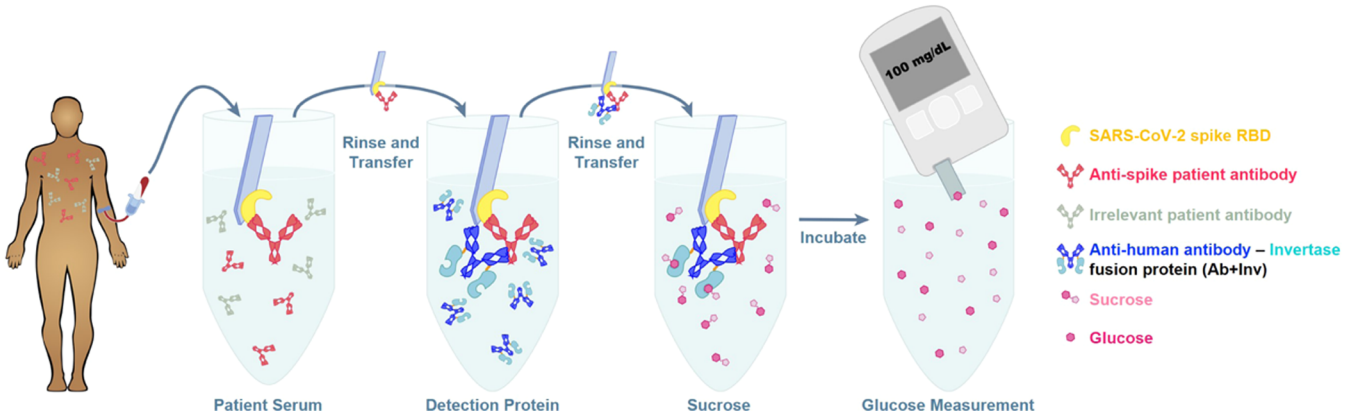

Figure 1. Schematic overview of the detection assay to quantify COVID-19-specific antibodies using a commercially available glucometer. A strip coated with SARS-CoV-2 spike protein RBD is incubated with patient serum, and RBD-specific antibodies bind to the strip. The strip is rinsed to remove any nonspecific antibodies and transferred to a solution containing Ab+Inv fusion protein, which binds to the patient antibody captured on the strip. The strip is again rinsed, transferred to a solution of sucrose, and incubated. The amount of sucrose converted to glucose is measured using a commercial glucometer and is proportional to the amount of the patient's antibodies in the serum.

vaccine-induced immunity and how these differences may impact the spread of disease. Finally, at an individual level, a point-of-care antibody serology diagnostic would allow patients to assess their personal degree of disease susceptibility, empowering them to make informed decisions concerning lifestyle and preventative care.

Benchmark commercial antibody detection assays achieve high sensitivity by entrapping immunoglobulins (Igs) from human samples between the target antigen and a detection antibody, which is typically conjugated to a reporter enzyme. The concentration of immunoglobulins in clinical specimens is then determined spectrophotometrically by quantifying the product of the enzymatic reaction, which is directly proportional to the number of "sandwiched" immunoglobulins. Although several enzyme reporters have been described in the literature,[12] current benchmark antibody assays use either horseradish peroxidase (HRP) or alkaline phosphatase (AP). These enzymes are easily isolated from plants (HRP)[13] or animal tissues (AP)[14] and achieve high catalytic rates (2600 and 850 s^{-1}, respectively),[12] leading to intense optical signal outputs. Due to these favorable properties, HRP- and AP-based enzyme-linked immunosorbent assays (ELISAs) remain the standard approach for serological testing.[15] Commercial ELISA instrumentation is available in an array of formats and scales, ranging from portable instruments (e.g., manufactured by Samsung, Alere, and Eurolyser Diagnostica) to high-throughput, multiplexed clinical analyzers (e.g., manufactured by Luminex).[15] However, the requirement for expensive high-quality optical equipment to achieve accurate antibody measurements often restricts the availability of such instruments to specialized laboratories. Translation of ELISA technology to the point of care has been demonstrated via lateral flow assays; however, mainstream lateral flow platforms are still essentially limited to qualitative results.[16] Companies and researchers in the field are working to democratize the availability of portable ELISA detectors,[17,18] but currently, the steep cost complicates broad adoption, highlighting the critical need to develop new, cost-effective diagnostic strategies that allow for detection and quantitative measurement of antibody titers at the point of care.

A rational strategy to achieve rapid, broadly deployable, and easily executable monitoring of antibody titers lies in coupling antibody assays with digital bioelectronic detectors, such as personal glucometers, which are commercially available to the population scale. Yi Lu and colleagues pioneered the concept of using glucometers as modular diagnostic devices,[19,20] highlighting the extensive clinical validation that over-the-counter glucometers have undergone in diabetes treatment, as well as their increasingly robust integration with mobile health solutions. By conjugating a detection aptamer to a reporter enzyme, Lu et al. coupled detection of several target molecules to the production of glucose, rather than traditional colorimetric or fluorogenic products utilized by ELISAs. The concentration of glucose, as measured by the glucometer, was thus directly proportional to the number of analyte molecules present in the clinical sample. Several enzymes have been proposed for this detection approach;[19] however, the biocatalyst invertase uniquely combines high catalytic rates (~1540 s^{-1}, comparable to HRP and AP), thermal stability (up to 80 °C), pH stability (pH = 3−6), and high specificity for the substrate sucrose.[21,22]

Invertase-mediated conversion of sucrose has been integrated into recent molecular diagnostics,[23−29] but the coupling of invertase and the detection molecule (e.g., antibody) has proved difficult. Some studies have avoided direct attachment by conjugating both the detection antibody and invertase to the same nanoparticle[23,24] or nanowire,[25] whereas others have used streptavidin as an intermediate and formed complexes of the biotinylated antibody and biotinylated invertase.[26] To avoid the steric issues that likely interfere with efficient chemical conjugation methods, invertase has been conjugated to a small nucleic acid aptamer.[27,28] Just one group has reported the direct, site-specific, enzyme-mediated conjugation of invertase to an antibody single-chain fragment (scFv),[29] and though this method had the advantage of ensuring a consistent ratio of invertase to the detection molecule, conjugation efficiency was found to be very low.

Here, we designed a genetic fusion protein comprised of an antibody against the Fc domain of human IgG (anti-hIgG) and the enzyme invertase. Our fusion protein overcomes the issues of inefficient and inconsistent chemical coupling of invertase to detection molecules, which has previously hindered the development of glucometer-based detection systems. Our engineered antibody−enzyme fusion protein (denoted Ab

https://doi.org/10.1021/jacs.2c02537
J. Am. Chem. Soc. XXXX, XXX, XXX−XXX

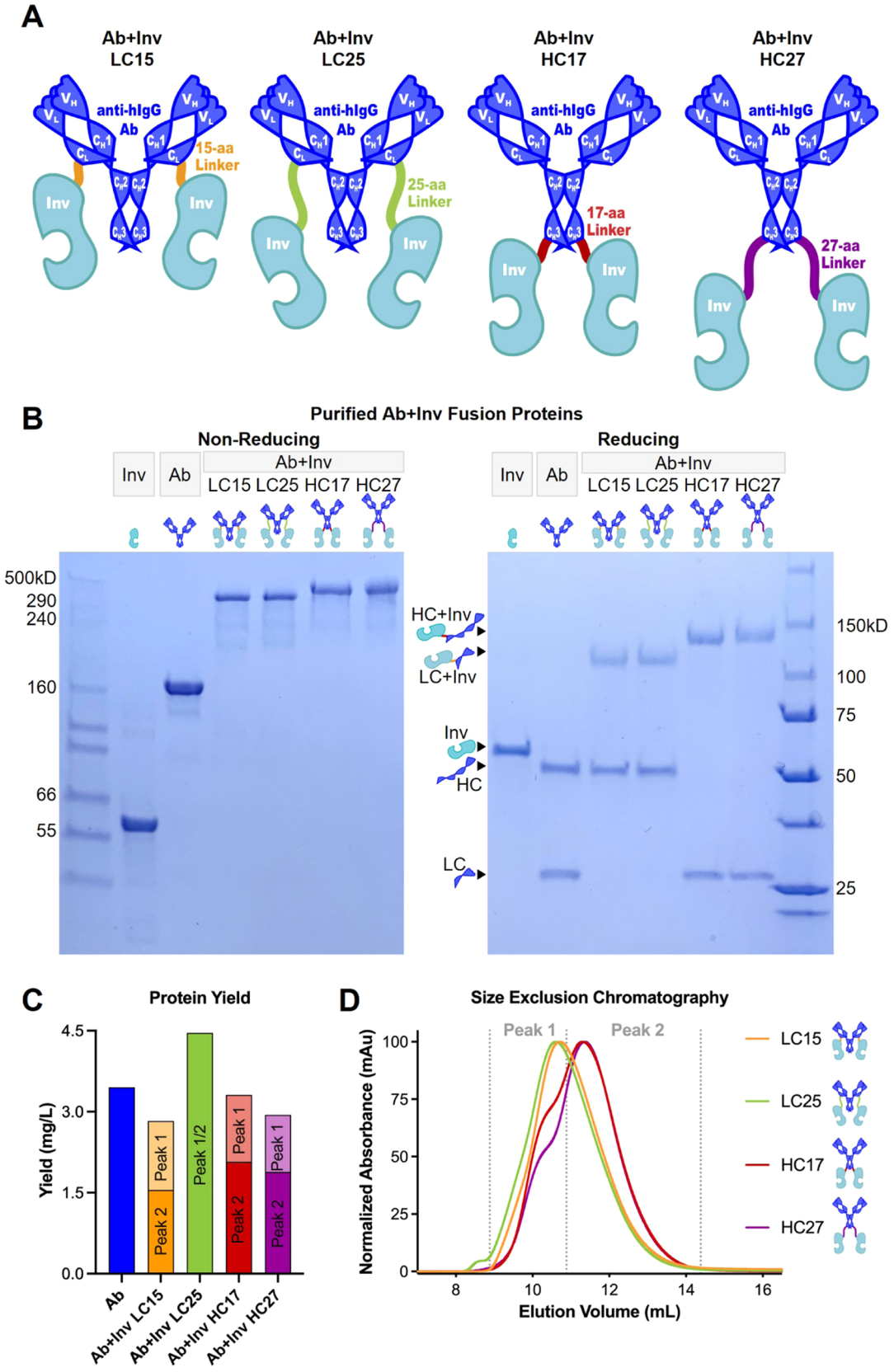

Figure 2. Design and purification of antibody−invertase (Ab+Inv) fusion proteins. (A) Schematic of Ab+Inv fusion proteins containing an antihuman IgG antibody. The C-terminus of the antibody light chain (LC) was tethered to the N-terminus of invertase via a flexible linker 15 or 25 amino acids in length (LC15 and LC25, respectively) or the C-terminus of the heavy chain (HC) is tethered to the N-terminus of invertase via a flexible linker 17 or 27 amino acids in length (HC17 and HC27, respectively). HC and LC variable and constant domains are labeled. (B) Ab+Inv fusion proteins migrate at slightly larger molecular weights (MW) than expected by SDS-PAGE. The unfused antibody (Ab) and invertase (Inv) alone run at the expected sizes under nonreducing (146 kDa for Ab and 62 kDa for Inv) and reducing (49 kDa for Ab HC, 24 kDa for Ab LC, and

https://doi.org/10.1021/jacs.2c02537
J. Am. Chem. Soc. XXXX, XXX, XXX−XXX

Figure 2. continued

62 kDa for Inv) conditions. Note that the samples for both SDS-PAGE gels were boiled to minimize the divergent migration of invertase and the fusion proteins relative to their expected molecular weights (62 kDa for invertase and ∼266 kDa for the Ab+Inv fusion proteins). The Ab+Inv fusion proteins run somewhat larger than their expected MW (∼266 kDa) under nonreducing conditions, as do the Inv-fused LC (∼84 kDa) and HC (∼110 kDa) under reducing conditions. (C) Yield per liter of transfected cells for each Ab+Inv fusion protein is shown compared to the yield of the unfused antibody (Ab). For LC15, HC17, and HC27, the yield from the pooled peak 1 is shown in a lighter shade and the yield from the pooled peak 2 is shown in the darker shade. Bar height reflects the total yield for both peaks. (D) Representative size-exclusion chromatography (SEC) traces for the four Ab+Inv fusion proteins are shown. The separately pooled fractions that were tested for LC15, HC17, and HC27 (peak 1 and peak 2) are indicated.

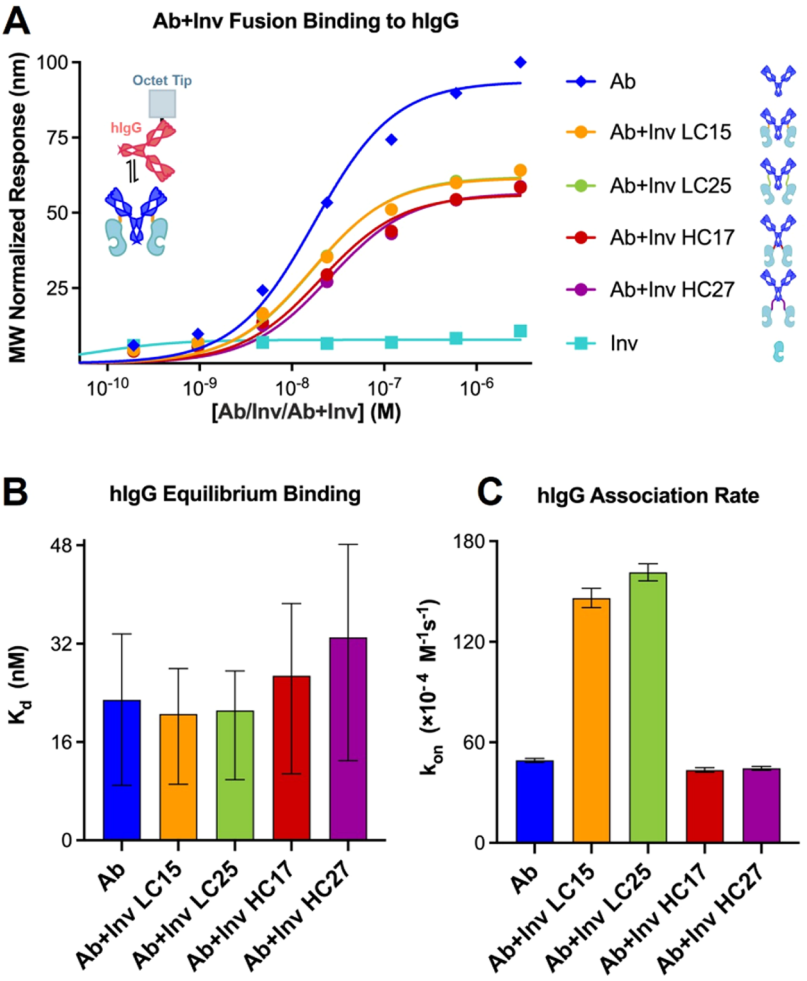

Figure 3. Ab+Inv fusion proteins bind hIgG with the same affinity as the unfused antibody. (A) Equilibrium BLI titrations of the soluble HP6017 antibody, Ab+Inv LC15, LC25, HC17, and HC27 against immobilized hIgG. Invertase (Inv) is included as a negative control. (B) K_D derived from the three-parameter curve fit of the equilibrium binding data in panel (A) is shown. (C) Association rate (k_{on}) generated from the kinetic BLI curve fit of the data in Figure S2, assuming a 1:1 binding model, is shown.

+Inv) was produced with high yields in a mammalian expression system, and the resulting construct fully preserved human IgG binding and catalytic activity relative to unmodified proteins. We validated that a strip-based assay (Figure 1), which employed this fusion protein, was effective in distinguishing between human samples that did or did not contain SARS-CoV-2-specific antibodies, with comparable sensitivity to gold-standard commercial ELISA-based detection methods. Given the rapid, robust, and broadly deployable nature of the system we developed, this platform promises to promote the understanding and containment of the SARS-CoV-2 virus. Furthermore, the versatile format allows for ready adaptation as a precision diagnostic to detect a wide range of diseases and medical conditions.

RESULTS

Design and Purification of Antihuman Antibody–Invertase Fusion Proteins (Ab+Inv). We produced four antihuman IgG–invertase fusion proteins (Ab+Inv, Figure 2A), which varied in the positioning and length of the peptide linkers connecting the antibody to two molecules of invertase. Fusion proteins were based on the antihuman IgG antibody HP6017, which binds the Fc domain of all human IgG isotypes.[30,31] The four fusion proteins were produced via transient transfection of human embryonic kidney (HEK)

https://doi.org/10.1021/jacs.2c02537
J. Am. Chem. Soc. XXXX, XXX, XXX−XXX

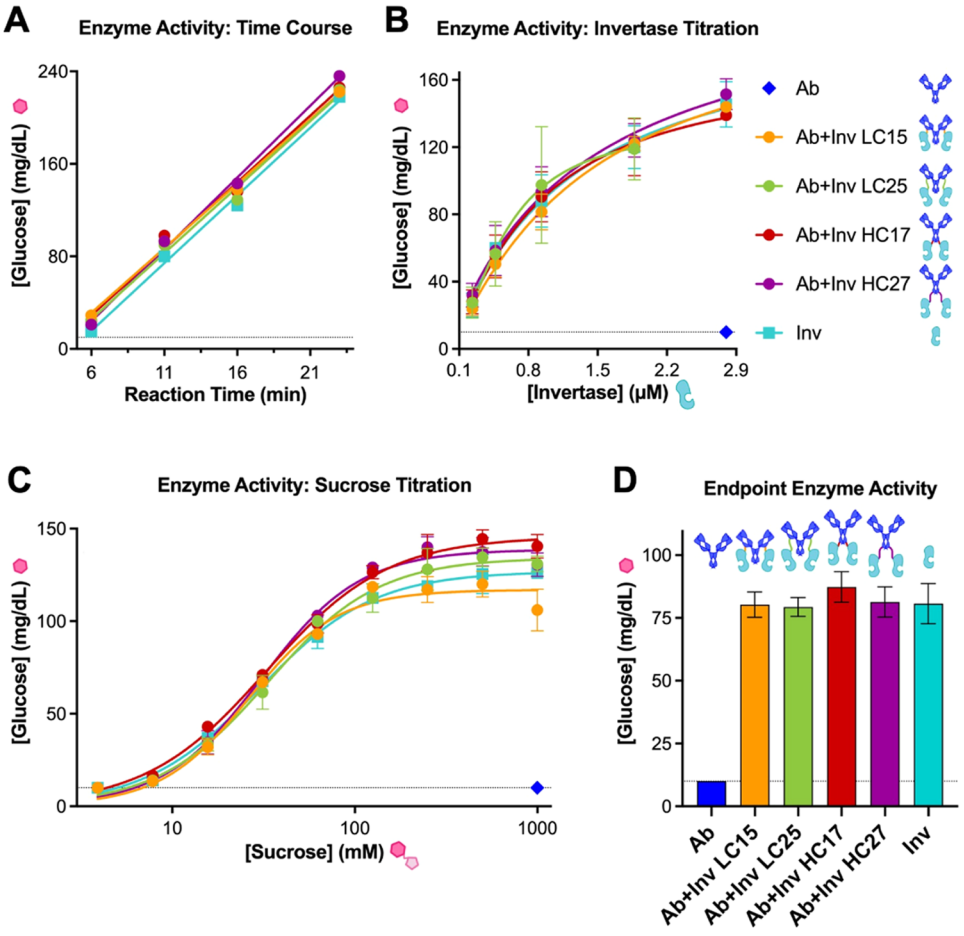

Figure 4. Ab+Inv fusion proteins exhibit equivalent catalytic activity to unfused invertase. (A) Ab+Inv fusion proteins or invertase (Inv) were incubated with 250 mM sucrose for 6 to 24 min. Concentrations of 166 nM Ab+Inv fusion proteins and 330 nM for Inv were used to achieve a molar equivalent amount of the enzyme, $n = 1$. (B) Various concentrations of unfused Ab, Ab+Inv fusion proteins, or Inv were incubated with 250 mM sucrose for 8 min. The concentration of the Ab+Inv fusion proteins is one-half of the invertase concentration shown on the x-axis, as each fusion protein contains two copies of invertase, $n = 2$. (C) Unfused Ab, Ab+Inv fusion proteins, or Inv were incubated with various concentrations of sucrose for 15 min. Concentrations of 166 nM Ab+Inv fusion proteins and 330 nM for Inv were used to achieve a molar equivalent amount of the enzyme, $n = 2$. (D) Unfused Ab, Ab+Inv fusion proteins, or Inv were incubated with 250 mM sucrose for 15 min. Concentrations of 166 nM Ab+Inv fusion proteins and 330 nM for Inv were used to achieve a molar equivalent amount of the enzyme, $n = 3$. The dotted lines in (A)−(D) indicate the limit of detection for the glucometer (10 mg/dL). Error bars indicate standard deviation in all panels.

293F cells. The fusion proteins ran slightly larger than their expected sizes (each ∼266 kDa), which was consistent with the observation that unboiled invertase runs larger than its predicted molecular weight of 62 kDa (Figures 2B and S1A−E). Accordingly, under reducing conditions, fusion proteins comprising invertase and a single light chain (LC) or heavy chain (HC) ran slightly larger than their predicted molecular weights (84 kDa for LC fusion proteins and 110 kDa for HC fusion proteins), whereas the unfused LC and HC ran as expected (Figure 2B). All Ab+Inv fusion proteins expressed robustly, with purified protein yields ranging from 2.8 to 4.5 mg/L of transfection, similar to the unfused antibody yield of 3.5 mg/L (Figure 2C). The four Ab+Inv fusion proteins showed similar profiles by size-exclusion chromatography (SEC), though the HC fusion proteins (HC17 and HC27) exhibited a discernable shoulder extending to the left of the main peak (denoted peak 1, Figure 2D). Moreover, earlier fractions of LC15, coinciding with peak 1, contained greater amounts of aggregate (Figure S1B). Interestingly, a comparison of the pooled peak 1 and peak 2 fractions from the HC and LC15 fusion proteins revealed similar activity (Figure S1F). Due to reduced aggregation, peak 2 of LC15, HC17, and HC27 was used for all subsequent characterization.

Validation of Ab+Inv Binding to Human IgG. To demonstrate that our Ab+Inv fusion proteins retained binding to the target antigen (i.e., human IgG), biolayer interferometry studies were performed. The four Ab+Inv fusion proteins showed similar human IgG binding properties relative to what was observed for the unfused antibody, with LC15 and LC25 showing a marginally higher affinity (Figure 3A,B, Table S1). The Ab+Inv fusion proteins showed slightly lower maximal binding levels (E_{max}) compared to the unfused antibody, presumably due to steric effects resulting from the increased size of the invertase fusion. Analysis of kinetic binding parameters further revealed that LC15 and LC25 had significantly higher association rates compared to both the unfused antibody and the HC fusion proteins (Figures 3C, S2, and Table S1). While the binding properties of all four Ab+Inv fusion proteins were very similar, these data suggested that the LC fusion proteins had slightly superior binding activity compared to the HC fusion proteins.

https://doi.org/10.1021/jacs.2c02537
J. Am. Chem. Soc. XXXX, XXX, XXX−XXX

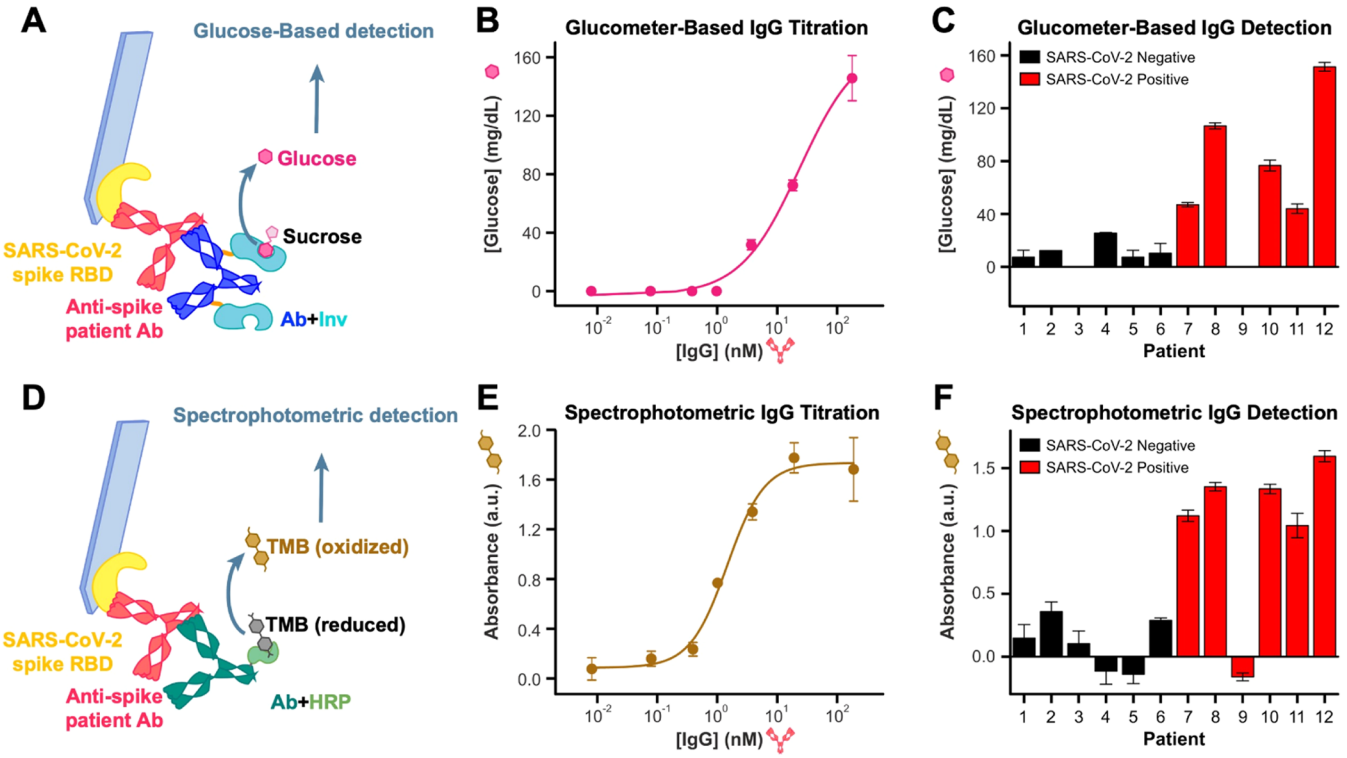

Figure 5. Glucometer-based immunoassay using Ab+Inv fusion protein detects the presence of SARS-CoV-2-targeted antibodies in patient samples. (A) Schematic of the detection workflow for the glucometer-based strip immunoassay, which detects sucrose conversion by Ab+Inv fusion protein LC15 in proportion to SARS-CoV-2 spike protein RBD-targeted antibodies in a test sample. (B) Platform shown in (A) was used to build calibration curves in 10% serum, detecting glucose readouts for various concentrations of the spiked anti-SARS-CoV-2 spike protein RBD antibody. The fitted single curve yields EC_{50} = 35 nM, with n = 3. The limit of detection (LOD) is 1.2 ± 0.2 nM. (C) This platform was used to measure anti-SARS-CoV-2 antibody titers in patient samples with known seroconversion status (TS1), with n = 3. (D) Schematic of the detection workflow for a benchmark spectrophotometric strip immunoassay, which detects tetramethylbenzidine (TMB) oxidation by horseradish peroxidase (HRP)-labeled anti-hIgG antibodies in proportion to SARS-CoV-2 spike protein RBD-targeted antibodies in a test sample. (E) The strategy shown in (D) was used to build calibration curves in 10% serum, detecting glucose readouts for various concentrations of spiked anti-SARS-CoV-2 spike protein RBD antibodies. The fitted single curve yields EC_{50} = 2 nM, with n = 3. The LOD is 0.8 ± 0.1 nM. (F) This strategy was used to measure anti-SARS-CoV-2 antibody titers in patient samples with known seroconversion status (TS1), with n = 3. Discrimination between positive and negative samples matched that of the glucometer-based assay. Error bars indicate standard deviation in all panels.

Validation of Ab+Inv Catalytic Activity. To determine whether our Ab+Inv fusion proteins preserved the catalytic activity of the component invertase enzyme, we implemented glucose conversion assays using a commercial glucometer. We compared the catalytic activity of the four Ab+Inv fusion proteins in solution by measuring the extent of glucose production after incubating the proteins with specified concentrations of sucrose. The four Ab+Inv fusion proteins achieved nearly identical enzymatic activity to the unfused invertase in time-course experiments (Figure 4A), enzyme titrations (Figure 4B), substrate (sucrose) titrations (Figure 4C), and endpoint activity measurements (Figure 4D). Enzymatic activity was not affected by concurrent binding to hIgG, as was demonstrated by endpoint experiments performed with a 2× molar excess of hIgG (Figure S3). While the overall enzymatic activities for each of the four Ab+Inv fusion proteins were very similar, LC25 exhibited greater variability for measurements near the middle of the dynamic range for the enzyme titrations (Figure 4B).

Development and Deployment of an Anti-SARS-CoV-2 Antibody Detection Assay. To demonstrate the diagnostic potential for our Ab+Inv fusion proteins, we sought to establish that they could accurately differentiate between patient samples that did or did not contain SARS-CoV-2-specific antibodies via a strip-based assay that would be amenable to point-of-care use (Figure 1). To build the assay, we designed plastic test strips (.stl file provided in the Supporting Information) that fit snugly inside 1.5 mL microcentrifuge tubes. The strips were fabricated using a CO_2 laser cutter from 2 mm thick poly(methyl methacrylate) sheets (example cuts shown in Figure S4). We coated the strips with established antifouling hydrogel technology to minimize nonspecific protein binding from patient samples to the surface.[32] The hydrogel was then functionalized with the receptor-binding domain (RBD) of the SARS-CoV-2 spike protein via covalent coupling using carbodiimide chemistry. We established the antigen loading and secondary antibody concentration that provided the highest assay sensitivity via spectrophotometric tests in phosphate-buffered saline (PBS, Figure S5A−C), consisting of HRP-modified, ELISA-validated antispike antibodies and tetramethylbenzidine (TMB)/hydrogen peroxide solutions. The resulting antigen-loaded strips can be stored in the buffer at 4 °C and are amenable for use in quantifying anti-SARS-CoV-2 antibodies in patient samples.

Our electrochemical immunoassay consisted of exposing the test strips to a series of binding and washing steps to ultimately produce a solution containing glucose in direct proportion to the number of anti-SARS-CoV-2 antibodies present in each

https://doi.org/10.1021/jacs.2c02537
J. Am. Chem. Soc. XXXX, XXX, XXX−XXX

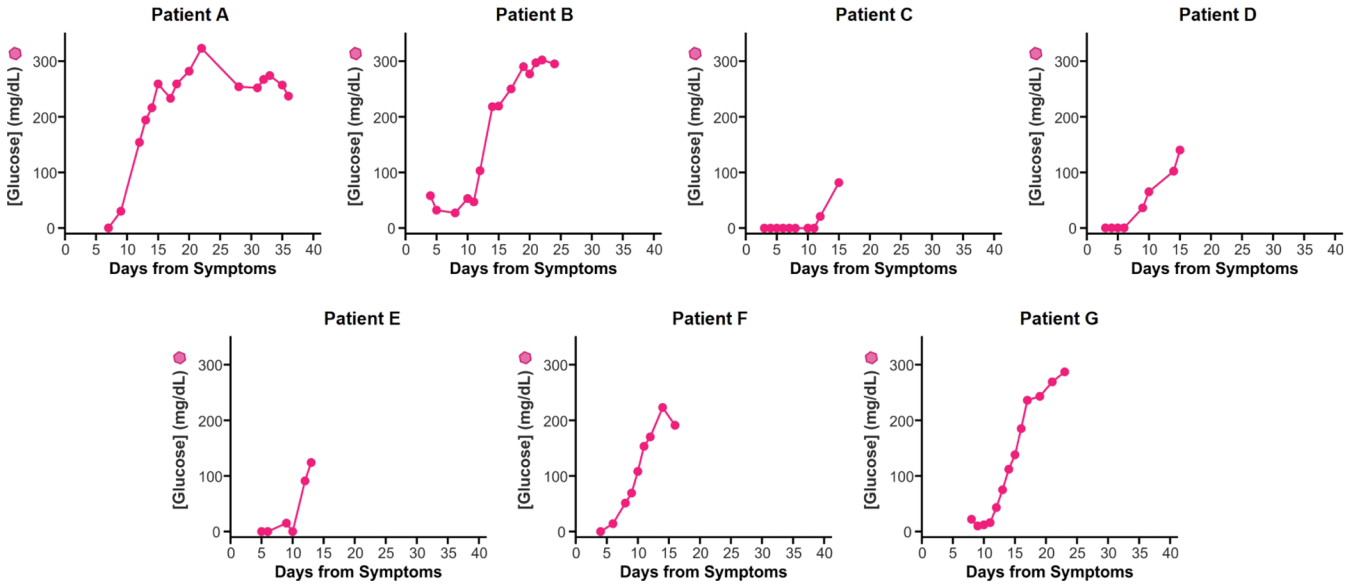

Figure 6. Glucometer-based immunoassay using Ab+Inv fusion protein enables monitoring of anti-SARS-CoV-2 antibody titers in hospitalized patients. A glucometer-based strip immunoassay was used to measure SARS-CoV-2 spike protein RBD-targeted antibody levels in samples from hospitalized patients with COVID-19 (TS2), $n = 1$. The glucometer assay consistently determined the emergence of anti-SARS-CoV-2 antibody responses at ∼10 days post symptom onset, and responses plateaued at ∼20 days post symptom onset in patients A, B, F, and G. Solid lines are included for visual clarity to highlight IgG titer trends.

sample (Figures 1 and 5A). Briefly, we first immersed the RBD-modified strips in either control or infected patient samples for 30 min to allow anti-SARS-CoV-2 spike protein RBD antibodies to bind, followed by a wash step. We then exposed the strips to Ab+Inv fusion protein solutions for 30 min so that the fusion protein would bind to the captured antibody on the strip, also followed by a wash. In the third step, we immersed the strips in 100 mM sucrose solution for 60 min to allow invertase to catalyze conversion to glucose, after which we removed the strips and determined the resulting glucose concentration using a commercial glucometer. The exact measurement protocol varied slightly depending on whether we performed control measurements using the spectrophotometric HRP/TMB reporter system, or the invertase/sucrose reporter system, as described in detail in the SI Methods section.

We first established which of our four Ab+Inv fusion proteins achieved the greatest sensitivity in strip-based immunoassays. To do this, we incubated the strips with an antispike antibody (13.6 nM), followed by exposure to saturating concentrations (0.1 μM) of each of the four Ab +Inv fusion proteins. Our results indicated that, under identical assay conditions, the LC fusion proteins produced ∼55% more glucose than the HC fusion proteins (Figure S6). Because the LC15 fusion protein achieved the highest generation of glucose, we selected this molecule for assay development. Then, we optimized the concentration of LC15 for the strip assay (Figure S5B) and subsequently built assay calibrations in PBS to establish the dynamic range of our reporter relative to spectrophotometric detection (Figure S7A,B). The detection range of both methods compared well, allowing us to proceed to clinical validation trials. For such trials, we accessed confirmed negative and positive patient blood samples from institutional biorepositories. We obtained two blinded training sample sets: **TS1** contained six confirmed negatives (from pre-pandemic Johns Hopkins Hospital emergency department patients) and six confirmed positives (from potential convalescent plasma donors who had prior RT-PCR confirmation of SARS-CoV-2 infection).[33] **TS2** consisted of 90 longitudinal samples (collected over time) from seven hospitalized SARS-CoV-2 RT-PCR-confirmed patients with known dates of symptom onset.[34] The antibody titers of both training sets were unknown to our study team until we performed a crossed examination against commercial ELISA measurements.

Using the LC15 fusion protein as the reporter, we sought to determine whether our glucometer-based immunoassays achieved similar discrimination of negative and positive samples from training set **TS1** relative to analogous colorimetric assays. To develop the assay framework to test this, we first comparatively evaluated the performance of the LC15/sucrose (Figure 5A) and HRP/TMB (Figure 5D) reporter systems built from strip-based assays using 10% commercial SARS-CoV-2 negative patient sera spiked with increasing concentrations of commercial anti-SARS-CoV-2 spike protein RBD IgGs. We observed strong assay responses at this dilution of the patient serum samples (using the spectrophotometric test, Figure S8); thus, a serum dilution of 10% was used for all subsequent assays. We used casein in all of the strip-based assays involving human serum to prevent nonspecific protein binding to the test strips, by incubating the strips into a casein solution at a concentration of 5% (w/w) for 1 h after immobilizing the RBD. However, for glucometer-based detection, casein was not added to human serum samples. Although the addition of a 5% w/w concentration of casein is common practice for ELISA-based detection to reduce nonspecific background signal,[35,36] we did not observe background in our assay, even in the absence of casein (Figure S9). Moreover, we observed a ∼2-fold improvement in the signal output of the glucometer-based assay when casein was not present, thus motivating exclusion of this reagent in our assay. We also optimized the strip incubation time with the sucrose solution (Figure S10). Based on our findings, incubation of the strips in serum without casein for binding

https://doi.org/10.1021/jacs.2c02537
J. Am. Chem. Soc. XXXX, XXX, XXX−XXX

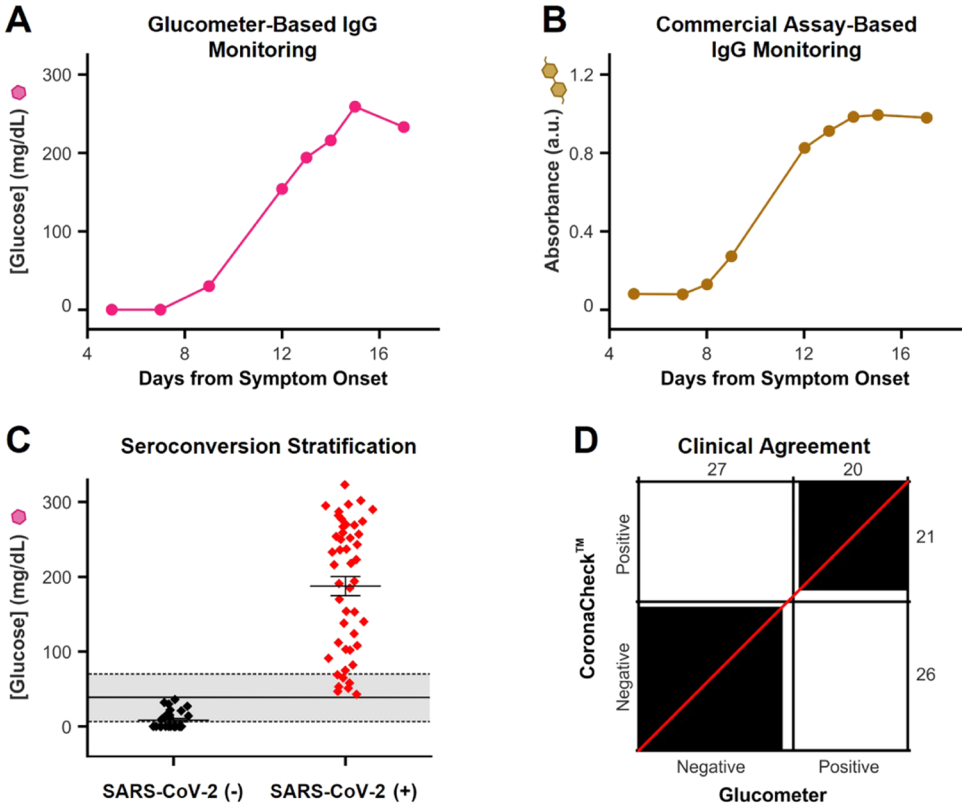

Figure 7. Robust clinical agreement observed between glucometer-based and commercial spectrophotometric immunoassays. (A) Longitudinal time course of SARS-CoV-2 spike protein RBD-targeted antibody levels in the hospitalized patient with COVID-19 (patient B from the TS2 cohort), as detected by the glucometer-based immunoassay using Ab+Inv fusion protein, with $n = 1$. (B) Longitudinal time-course of SARS-CoV-2 spike protein RBD-targeted antibody levels in the hospitalized patient with COVID-19 (patient B from the TS2 cohort), as detected by a commercial spectrophotometric assay (Epitope Diagnostics), with $n = 1$. (C) To establish a seroconversion threshold for the glucometer-based assay, we computed the average and standard deviation (gray shaded areas) of the glucose output generated by five confirmed SARS-CoV-2 negative samples, obtaining a seroconversion cutoff of 39 ± 32 ng/mL. Extrapolating this threshold to all the data from the TS2 cohort, we were able to accurately stratify by seroconversion status. The short horizontal lines represent the mean and ± standard errors for the two groups. (D) Agreement chart generated using the Bangdiwala method,[38] comparing glucometer-based measurements with a commercial spectrophotometric assay (Coronacheck). A 95% positive and a 96% negative percent agreement were observed.

to patient antibodies and in sucrose solution for 60 min during detection was selected. The resulting dose−response curves indicated that the HRP/TMB reporter assay achieved higher sensitivity (EC_{50} ∼ 2 nM, Figure 5E) and the signal output plateaued at lower concentrations of anti-SARS-CoV-2 spike protein RBD IgG (∼13.6 nM) compared to the LC15/sucrose reporter system (EC_{50} ∼ 35 nM, plateau at >150 nM, Figure 5B). Note that the assay readouts reflect two binding events (the primary antibody binding to the spike protein and the secondary antibody binding to the primary antibody), as well as enzyme-mediated catalysis. The sensitivity differences between the HRP/TMB reporter and LC15/sucrose reporter systems were not unexpected, as the catalytic rate of HRP is approximately two-fold faster than that of the invertase in LC15. Despite this discrepancy, when we challenged both systems with **TS1** samples, they exhibited the comparable capacity to distinguish between all confirmed negative and positive specimens (Figure 5C vs F). Notably, the apparently false-negative data obtained for patient 9 was later confirmed to be a true negative via commercial ELISA assays (Epitope Diagnostics (EDI) COVID-19), and the sample corresponds to a convalescent patient with unusually low antibody titers.

We next examined whether the LC15 fusion protein would enable accurate glucometer-based monitoring of immune responses in longitudinal samples. To this end, we exposed our test strips to samples from training set **TS2** and compared results against the clinically used EDI COVID-19 and CoronaCheck immunoassays. Note that the EDI assay employs the nucleocapsid of SARS-CoV-2 as the target antigen, whereas the CoronaCheck assay, like our glucometer-based immunoassays, employs the RBD protein. Our glucometer-based measurements showed an onset of anti-SARS-CoV-2 IgGs ∼10 days after the first record of symptoms across patient samples (Figure 6). In addition, for the three sample sets with sufficient measurement points to identify a plateau in antibody responses, we characterized such a plateau at ∼20 days post infection. This finding was in close agreement with results from commercial antibody assays (Figures S11 and S12) and demonstrated superior seroconversion resolution over, for example, lateral flow immunoassays.[34,37] Moreover, in a side-by-side comparison of LC15/sucrose (Figure 7A) and EDI COVID-19 (Figure 7B) measurements using the same patient samples (**TS2**), the resulting time-course profiles were similar. These results highlight the potential value that our fusion protein reporter and glucometer-based immunoassay have in monitoring the development and maintenance of immunity temporally, across populations, without the need for spectrophotometric or other optical equipment.

https://doi.org/10.1021/jacs.2c02537
J. Am. Chem. Soc. XXXX, XXX, XXX−XXX

Two critical figures of merit for new immunoassays are the positive (PPA) and negative percent agreements (NPA) relative to benchmark commercial immunoassays. To determine the PPA and NPA for our glucometer-based assay, we first established a positive seroconversion threshold based on the average response of our assay to confirmed negative specimens (Figure 7C). Specifically, we measured the output of our assay when challenged with four pre-pandemic samples from hospitalized patients plus one commercial sample pooled from 10 healthy donors. We established the seroconversion threshold for our glucometer-based assay by computing the mean and standard deviation of measurements from healthy donor samples, 39 ± 32 mg/dL (black line and shaded areas, respectively, in Figure 7C), to set the background level, above which all measurements were considered to be seroconversion positive. Applying this cutoff to our measurements over all longitudinal samples, we deemed 64% (49 samples) to be positive and 36% (27 samples) to be negative. The accuracy of this determination can be better demonstrated by directly comparing glucometer-based immunoassay determinations relative to CoronaCheck measurements. The resulting agreement chart[38] (Figure 7D) reported a PPA = 95% (20/21 × 100) and NPA = 96% (26/27 × 100), demonstrating again that our glucometer-based immunoassays achieve similar performance relative to benchmark spectrophotometric assays currently in clinical use. We include side-by-side comparisons of assay time (Table S2) and estimated cost per test (Table S3) between our glucometer-based detection assay and two commercial spectrophotometric kits to further illustrate the competitive value of our technology.

DISCUSSION

We report here a novel fusion protein comprising anti-hIgG and two invertase molecules, which can be used as an electrochemical reporter for rapid and robust glucometer-based immunoassays. By virtue of being expressed as a single protein from a eukaryotic cell line, our fusion protein overcomes purification and heterogeneity challenges related to the post-expression chemical coupling of enzymatic reporters to detection antibodies. Specifically, we were able to express four antihuman antibody−invertase fusion proteins (Ab+Inv), all of which were successfully expressed in mg/L yields (Figure 2) and retained the binding affinity and catalytic activity of the respective unconjugated parent proteins (Figures 3 and 4). The Ab+Inv fusion protein that showed the best functional activity, denoted LC15, enables the possibility to perform immunoassays using widely available glucometers as detectors, obviating the need for expensive and specialized spectrophotometric or optical instrumentation and reducing the level of technical skill required to perform the test. We note that the dynamic range of the glucometer used in this study (Nova Biomedical, 10−600 mg/dL) is comparable to that of other commercially available glucometers that follow 2020 FDA guidelines;[39] thus, our reporter fusion protein can be readily used across a range of glucometer brands. Moreover, because LC15 binds to the Fc region of all human IgG isotypes, the protein can be immediately used as a secondary antibody reporter for a vast range of antibody assays, in a similar fashion as the benchmark HRP/TMB system.

To illustrate the ability of LC15 to support accurate antibody measurements in clinical specimens, we developed a plastic-strip-based immunoassay that quantifies anti-SARS-CoV-2 antibodies as a model case for our glucose-based detection system. We then validated our platform by performing glucometer-based antibody assays using two different clinical blood sample training sets, one consisting of pre-pandemic negative samples and samples from SARS-CoV-2 positive patients and a second set consisting of longitudinal samples from hospitalized, COVID-19-confirmed patients. Based on studies using both training sets, our glucometer-based immunoassays performed comparably against either an identical HRP/TMB-based test performed in our lab (Figure 5) or commercial immunoassays that are currently in clinical use (Figures 6 and 7). Our results demonstrate remarkable accuracy and agreement with commercially available immunoassays. We also note that optimization of the anti-hIgG antibody in LC15 through affinity maturation could further improve the sensitivity and performance of our assay. Additional optimization could entail engineering invertase to have optimal activity at room temperature; the optimal catalytic conditions for invertase are incompatible with our assay, as it would be performed at the point of care. While the performance of invertase in our assay was sufficient under point-of-care conditions, catalytic optimization at room temperature would enhance the sensitivity of the assay and decrease the amount of time required for measurements. With increased sensitivity, it is likely that our diagnostic will be translatable for use with other types of patient samples, such as nasopharyngeal swab[40] or saliva.

The Ab+Inv fusion protein LC15 represents an emerging class of reporter proteins. While antibodies and other binding molecules have previously been chemically conjugated to invertase, to our knowledge, this is the first example wherein invertase has been attached directly through genetic fusion. Importantly, the yields observed for Ab+Inv LC15 were very similar to the yield for the unfused antibody (Figure 2C), indicating that the cost of large-scale production of the fusion would be similar to that for the antibody alone. While LC15 did appear to have more aggregate in peak 1, this aggregate did not impact binding or enzymatic activity, and these aggregates could likely be eliminated through optimization of transfection conditions. Encouragingly, LC15 eluted as a monodisperse peak via SEC, suggesting that high-purity manufacturing with limited attrition will be feasible. Moreover, as invertase is genetically fused to the antibody, we have eliminated additional chemical conjugation steps, which can be laborious and inconsistent and require additional purification to remove unconjugated protein, as well as quality confirmation. Furthermore, chemical conjugation methods are inherently stochastic, meaning that the number of invertase molecules conjugated to the antibody will unavoidably vary, whereas in our approach, the stoichiometry is fixed, which ensures high consistency between batches.

More broadly, this study represents one of the first instances in which a full-length antibody is genetically fused to an enzyme for the purposes of detection. The vast majority of previous work has generated scFv−enzyme fusion proteins[41−46] or fragment antigen-binding (Fab)−enzyme fusion proteins.[47,48] scFvs and Fabs contain only one antigen-binding site per molecule and thus do not benefit from the avidity advantage afforded by the two binding sites in a full-length antibody. To our knowledge, only one platform has been developed to produce enzymes that are genetically fused to full-length antibodies, specifically a fusion protein scaffold linking an enzyme to IgM, yielding a highly multimeric antibody−enzyme pentamer.[49] While the pentameric structure

https://doi.org/10.1021/jacs.2c02537
J. Am. Chem. Soc. XXXX, XXX, XXX−XXX

of IgM provides a dramatic avidity enhancement, naturally occurring IgMs generally have very low affinity compared to IgGs and are notoriously difficult to produce.[50,51] As such, our full-length IgG formulation leverages the multimeric avidity advantage while avoiding losses in yield, making it an ideal candidate for large-scale production.

The low technical requirements and low production cost for our Ab+Inv fusion protein will allow the proposed glucometer-based diagnostic platform to be employed for testing far greater numbers of people on a global scale, including those who do not have access to medical facilities with advanced testing capabilities. It will also empower serial testing, which combined with the number and diversity of people being tested will provide needed high-quality data to impart a clear and detailed understanding of the longevity of immune protection that is provided from vaccination and natural infection, as well as protection against emerging variants of concern. Specifically, straightforward substitution of the RBD with variant RBDs can test for antibodies that are protective against emerging variants, and substitution of the RBD with nucleocapsid (N) or membrane (M) proteins can inform whether patients have been previously infected with the SARS-CoV-2 virus. Moreover, replacing the SARS-CoV-2 RBD with another antigen from another infectious disease, a cancer diagnostic antigen, or a self-antigen associated with autoimmune diseases would allow this diagnostic to be implemented as a test for immunity to a large number of medical conditions and for longitudinal monitoring of disease control or progression. Altogether, the results of this study combined with the modularity of this technology highlight the potential value of our glucometer-based antibody detection approach for population-scale monitoring of immune responses to address the COVID-19 pandemic and a host of other biomedical applications. Further device development efforts will focus on simplifying the detection scheme so that the fusion protein and other reagents can be integrated into a portable, user-friendly, point-of-need detection platform.

■ ASSOCIATED CONTENT

Supporting Information

The Supporting Information is available free of charge at https://pubs.acs.org/doi/10.1021/jacs.2c02537.

Materials and methods, supplementary figures and tables (PDF)

Test strip design file (ZIP)

■ AUTHOR INFORMATION

Corresponding Authors

Jamie B. Spangler − *Department of Biomedical Engineering, Johns Hopkins University, Baltimore, Maryland 21218, United States; Department of Chemical and Biomolecular Engineering, Johns Hopkins University, Baltimore, Maryland 21218, United States; Translational Tissue Engineering Center, Bloomberg−Kimmel Institute for Cancer Immunotherapy, Sidney Kimmel Comprehensive Cancer Center, and Department of Ophthalmology, Wilmer Eye Institute, Johns Hopkins University School of Medicine, Baltimore, Maryland 21231, United States; Department of Oncology, Johns Hopkins University School of Medicine, Baltimore, Maryland 21205, United States;* orcid.org/0000-0001-8187-3732; Email: jamie.spangler@jhu.edu

Netzahualcóyotl Arroyo-Currás − *Department of Pharmacology and Molecular Sciences, Johns Hopkins University School of Medicine, Baltimore, Maryland 21205, United States; Department of Chemical and Biomolecular Engineering, Johns Hopkins University, Baltimore, Maryland 21218, United States;* orcid.org/0000-0002-2740-6276; Email: netzarroyo@jhmi.edu

Authors

Elissa K. Leonard − *Department of Biomedical Engineering, Johns Hopkins University, Baltimore, Maryland 21218, United States; Translational Tissue Engineering Center, Johns Hopkins University School of Medicine, Baltimore, Maryland 21231, United States*

Miguel Aller Pellitero − *Department of Pharmacology and Molecular Sciences, Johns Hopkins University School of Medicine, Baltimore, Maryland 21205, United States;* orcid.org/0000-0001-8739-2542

Boris Juelg − *Ragon Institute of MGH, MIT, and Harvard, Cambridge, Massachusetts 02139, United States*

Complete contact information is available at: https://pubs.acs.org/10.1021/jacs.2c02537

Author Contributions

◆E.K.L. and M.A.P. equally contributed to this work.

Funding

The authors acknowledge support from the Sherrilyn and Ken Fisher Center for Environmental Infectious Diseases, Division of Infectious Diseases of the Johns Hopkins University School of Medicine. Its contents are solely the responsibility of the authors and do not necessarily represent the official view of the Fisher Center or Johns Hopkins University School of Medicine. The authors also acknowledge support from the Emerson Collective Cancer Research Fund and a Johns Hopkins University Provost COVID-19 Research Response grant. E.K.L. is supported by NIH Training Grant K12 GM123914. The authors thank Dr. Jarrid Legere and Nova Biomedical for donating glucometers, glucose strips, and glucose standards in support of this project. The authors also thank Drs. Oliver Laeyendecker, Owen Baker, and Andrea Cox for performing spectrophotometric measurements on clinical specimens using commercial ELISA platforms in support of this work.

Notes

The authors declare no competing financial interest.

■ REFERENCES

(1) Goudsmit, J. The Paramount Importance of Serological Surveys of SARS-CoV-2 Infection and Immunity. *Eur. J. Epidemiol.* **2020**, *35*, 331−333.

(2) Theel, E. S.; Slev, P.; Wheeler, S.; Couturier, M. R.; Wong, S. J.; Kadkhoda, K. The Role of Antibody Testing for SARS-CoV-2: Is There One? *J. Clin. Microbiol.* **2020**, *58*, e00797-20.

(3) Bartsch, Y. C.; Fischinger, S.; Siddiqui, S. M.; Chen, Z.; Yu, J.; Gebre, M.; Atyeo, C.; Gorman, M. J.; Zhu, A. L.; Kang, J.; Burke, J. S.; Slein, M.; Gluck, M. J.; Beger, S.; Hu, Y.; Rhee, J.; Petersen, E.; Mormann, B.; Aubin, M. deS.; Hasdianda, M. A.; Jambaulikar, G.; Boyer, E. W.; Sabeti, P. C.; Barouch, D. H.; Julg, B. D.; Musk, E. R.; Menon, A. S.; Lauffenburger, D. A.; Nilles, E. J.; Alter, G. Discrete SARS-CoV-2 Antibody Titers Track with Functional Humoral Stability. *Nat. Commun.* **2021**, *12*, No. 1018.

(4) Feng, S.; Phillips, D. J.; White, T.; Sayal, H.; Aley, P. K.; Bibi, S.; Dold, C.; Fuskova, M.; Gilbert, S. C.; Hirsch, I.; Humphries, H. E.; Jepson, B.; Kelly, E. J.; Plested, E.; Shoemaker, K.; Thomas, K. M.;

Vekemans, J.; Villafana, T. L.; Lambe, T.; Pollard, A. J.; Voysey, M.; the Oxford COVID Vaccine Trial Group. Correlates of Protection against Symptomatic and Asymptomatic SARS-CoV-2 Infection. *Nat. Med.* **2021**, *27*, 2032−2040.
(5) Chen, Y.; Tong, P.; Whiteman, N. B.; Moghaddam, A. S.; Zuiani, A.; Habibi, S.; Gautam, A.; Xiao, T.; Cai, Y.; Chen, B.; Wesemann, D. R. Differential Antibody Dynamics to SARS-CoV-2 Infection and Vaccination *bioRxiv*, DOI: 10.1101/2021.09.09.459504.
(6) Khoury, D. S.; Cromer, D.; Reynaldi, A.; Schlub, T. E.; Wheatley, A. K.; Juno, J. A.; Subbarao, K.; Kent, S. J.; Triccas, J. A.; Davenport, M. P. Neutralizing Antibody Levels Are Highly Predictive of Immune Protection from Symptomatic SARS-CoV-2 Infection. *Nat. Med.* **2021**, *27*, 1205−1211.
(7) Wei, J.; Stoesser, N.; Matthews, P. C.; Ayoubkhani, D.; Studley, R.; Bell, I.; Bell, J. I.; Newton, J. N.; Farrar, J.; Diamond, I.; Rourke, E.; Howarth, A.; Marsden, B. D.; Hoosdally, S.; Jones, E. Y.; Stuart, D. I.; Crook, D. W.; Peto, T. E. A.; Pouwels, K. B.; Eyre, D. W.; Walker, A. S.; the COVID-19 Infection Survey team. Antibody Responses to SARS-CoV-2 Vaccines in 45,965 Adults from the General Population of the United Kingdom. *Nat Microbiol* **2021**, *6*, 1140−1149.
(8) Amanat, F.; Stadlbauer, D.; Strohmeier, S.; Nguyen, T. H. O.; Chromikova, V.; McMahon, M.; Jiang, K.; Arunkumar, G. A.; Jurczyszak, D.; Polanco, J.; Bermudez-Gonzalez, M.; Kleiner, G.; Aydillo, T.; Miorin, L.; Fierer, D. S.; Lugo, L. A.; Kojic, E. M.; Stoever, J.; Liu, S. T. H.; Cunningham-Rundles, C.; Felgner, P. L.; Moran, T.; García-Sastre, A.; Caplivski, D.; Cheng, A. C.; Kedzierska, K.; Vapalahti, O.; Hepojoki, J. M.; Simon, V.; Krammer, F. A Serological Assay to Detect SARS-CoV-2 Seroconversion in Humans. *Nat. Med.* **2020**, *26*, 1033−1036.
(9) Mendrone-Junior, A.; Dinardo, C. L.; Ferreira, S. C.; Nishya, A.; Salles, N. A.; Almeida Neto, C.; Hamasaki, D. T.; Facincani, T.; Oliveira Alves, L. B.; Machado, R. R. G.; Araujo, D. B.; Durigon, E. L.; Rocha, V.; Sabino, E. C. Correlation between SARS-COV-2 Antibody Screening by Immunoassay and Neutralizing Antibody Testing. *Transfusion* **2021**, *61*, 1181−1190.
(10) Oh, H.; Ahn, H.; Tripathi, A. A Closer Look into FDA-EUA Approved Diagnostic Techniques of Covid-19. *ACS Infect. Dis.* **2021**, *7*, 2787−2800.
(11) Lee, C. Y.-P.; Lin, R. T. P.; Renia, L.; Ng, L. F. P. Serological Approaches for COVID-19: Epidemiologic Perspective on Surveillance and Control. *Front. Immunol.* **2020**, *11*, 879.
(12) Porstmann, B.; Porstmann, T.; Nugel, E.; Evers, U. Which of the Commonly Used Marker Enzymes Gives the Best Results in Colorimetric and Fluorimetric Enzyme Immunoassays: Horseradish Peroxidase, Alkaline Phosphatase or β-Galactosidase? *J. Immunol. Methods* **1985**, *79*, 27−37.
(13) Gundinger, T.; Spadiut, O. A Comparative Approach to Recombinantly Produce the Plant Enzyme Horseradish Peroxidase in *Escherichia coli*. *J. Biotechnol.* **2017**, *248*, 15−24.
(14) Lewis, T. L.; Roth, K. A. Immunohistochemical Detection Methods. In *Pathobiology of Human Disease*, Elsevier, 2014; pp https://doi.org/10.1016/B978-0-12-386456-7.07405-0 pp 3829−3840.
(15) Vashist, S. K.; Luong, J. H. T. Enzyme-Linked Immunoassays. In *Handbook of Immunoassay Technologies*; Elsevier, 2018; pp 97−127.
(16) Moshe, M.; Daunt, A.; Flower, B.; Simmons, B.; Brown, J. C.; Frise, R.; Penn, R.; Kugathasan, R.; Petersen, C.; Stockmann, H.; Ashby, D.; Riley, S.; Atchison, C.; Taylor, G. P.; Satkunarajah, S.; Naar, L.; Klaber, R.; Badhan, A.; Rosadas, C.; Marchesin, F.; Fernandez, N.; Sureda-Vives, M.; Cheeseman, H.; O'Hara, J.; Shattock, R.; Fontana, G.; Pallett, S. J. C.; Rayment, M.; Jones, R.; Moore, L. S. P.; Ashrafian, H.; Cherapanov, P.; Tedder, R.; McClure, M.; Ward, H.; Darzi, A.; Elliott, P.; Cooke, G. S.; Barclay, W. S. SARS-CoV-2 Lateral Flow Assays for Possible Use in National Covid-19 Seroprevalence Surveys (React 2): Diagnostic Accuracy Study. *BMJ* **2021**, n423.
(17) Nguyen, V.-T.; Song, S.; Park, S.; Joo, C. Recent Advances in High-Sensitivity Detection Methods for Paper-Based Lateral-Flow Assay. *Biosens. Bioelectron.* **2020**, *152*, No. 112015.
(18) Urusov, A. E.; Zherdev, A. V.; Dzantiev, B. B. Towards Lateral Flow Quantitative Assays: Detection Approaches. *Biosensors* **2019**, *9*, 89.
(19) Lan, T.; Zhang, J.; Lu, Y. Transforming the Blood Glucose Meter into a General Healthcare Meter for in Vitro Diagnostics in Mobile Health. *Biotechnol. Adv.* **2016**, *34*, 331−341.
(20) Xiang, Y.; Lu, Y. Using Personal Glucose Meters and Functional DNA Sensors to Quantify a Variety of Analytical Targets. *Nature Chem* **2011**, *3*, 697−703.
(21) Chávez, F. P.; Rodriguez, L.; Díaz, J.; Delgado, J. M.; Cremata, J. A. Purification and Characterization of an Invertase from Candida Utilis: Comparison with Natural and Recombinant Yeast Invertases. *J. Biotechnol.* **1997**, *53*, 67−74.
(22) Gangadhara; Ramesh Kumar, P.; Prakash, V. Influence of Polyols on the Stability and Kinetic Parameters of Invertase from Candida Utilis: Correlation with the Conformational Stability and Activity. *Protein J.* **2008**, *27*, 440−449.
(23) Joo, J.; Kwon, D.; Shin, H. H.; Park, K.-H.; Cha, H. J.; Jeon, S. A Facile and Sensitive Method for Detecting Pathogenic Bacteria Using Personal Glucose Meters. *Sens. Actuators, B* **2013**, *188*, 1250−1254.
(24) Li, L.; Liang, D.; Guo, W.; Tang, D.; Zeng, Y. Antibody-invertase Cross-linkage Nanoparticles: A New Signal Tag for Point-of-care Immunoassay of Alpha-fetoprotein for Hepatocellular Carcinoma with Personal Glucometer. *Electroanalysis* **2021**, *34*, 246−251.
(25) Lin, J.; Tang, D. Glucometer-Based Signal Readout for a Portable Low-Cost Electrochemical Immunoassay Using Branched Platinum Nanowires. *Anal. Methods* **2016**, *8*, 4069−4074.
(26) Xiang, Y.; Lu, Y. Portable and Quantitative Detection of Protein Biomarkers and Small Molecular Toxins Using Antibodies and Ubiquitous Personal Glucose Meters. *Anal. Chem.* **2012**, *84*, 4174−4178.
(27) Wang, Q.; Liu, F.; Yang, X.; Wang, K.; Wang, H.; Deng, X. Sensitive Point-of-Care Monitoring of Cardiac Biomarker Myoglobin Using Aptamer and Ubiquitous Personal Glucose Meter. *Biosens. Bioelectron.* **2015**, *64*, 161−164.
(28) Zhang, S.; Luan, Y.; Xiong, M.; Zhang, J.; Lake, R.; Lu, Y. DNAzyme Amplified Aptasensing Platform for Ochratoxin A Detection Using a Personal Glucose Meter. *ACS Appl. Mater. Interfaces* **2021**, *13*, 9472−9481.
(29) Ismail, N. F.; Lim, T. S. Site-Specific ScFv Labelling with Invertase via Sortase A Mechanism as a Platform for Antibody-Antigen Detection Using the Personal Glucose Meter. *Sci. Rep.* **2016**, *6*, 19338.
(30) Jefferis, R.; Reimer, C. B.; Skvaril, F.; de Lange, G.; Ling, N. R.; Lowe, J.; Walker, M. R.; Phillips, D. J.; Aloisio, C. H.; Wells, T. W.; et al. Evaluation of Monoclonal Antibodies Having Specificity for Human IgG Sub-Classes: Results of an IUIS/WHO Collaborative Study. *Immunol. Lett.* **1985**, *10*, 223−252.
(31) Evaluation of Thirty-One Mouse Monoclonal Antibodies to Human IgG Epitopes|Hybridoma. https://www.liebertpub.com/doi/10.1089/hyb.1984.3.263 (accessed Feb 19, 2022).
(32) Sabaté del Río, J.; Henry, O. Y. F.; Jolly, P.; Ingber, D. E. An Antifouling Coating That Enables Affinity-Based Electrochemical Biosensing in Complex Biological Fluids. *Nat. Nanotechnol.* **2019**, *14*, 1143−1149.
(33) Patel, E. U.; Bloch, E. M.; Clarke, W.; Hsieh, Y.-H.; Boon, D.; Eby, Y.; Fernandez, R. E.; Baker, O. R.; Keruly, M.; Kirby, C. S.; Klock, E.; Littlefield, K.; Miller, J.; Schmidt, H. A.; Sullivan, P.; Piwowar-Manning, E.; Shrestha, R.; Redd, A. D.; Rothman, R. E.; Sullivan, D.; Shoham, S.; Casadevall, A.; Quinn, T. C.; Pekosz, A.; Tobian, A. A. R.; Laeyendecker, O. Comparative Performance of Five Commercially Available Serologic Assays To Detect Antibodies to SARS-CoV-2 and Identify Individuals with High Neutralizing Titers. *J. Clin. Microbiol.* **2021**, *59*, e02257−20.
(34) Conklin, S. E.; Martin, K.; Manabe, Y. C.; Schmidt, H. A.; Miller, J.; Keruly, M.; Klock, E.; Kirby, C. S.; Baker, O. R.; Fernandez, R. E.; Eby, Y. J.; Hardick, J.; Shaw-Saliba, K.; Rothman, R. E.; Caturegli, P. P.; Redd, A. D.; Tobian, A. A. R.; Bloch, E. M.; Larman,

https://doi.org/10.1021/jacs.2c02537
J. Am. Chem. Soc. XXXX, XXX, XXX−XXX

H. B.; Quinn, T. C.; Clarke, W.; Laeyendecker, O. Evaluation of Serological SARS-CoV-2 Lateral Flow Assays for Rapid Point-of-Care Testing. *J. Clin. Microbiol.* **2021**, *59*, e02020-20.
(35) Thermo Scientific *ELISA Technical Guide and Protocols*; Tech Tip; 65Thermo Scientific, 2010.
(36) Pratt, R. P.; Roser, B. *Comparison of Blocking Agents for ELISA*; Application NoteThermo Scientific, 2014.
(37) Whitman, J. D.; Hiatt, J.; Mowery, C. T.; Shy, B. R.; Yu, R.; Yamamoto, T. N.; Rathore, U.; Goldgof, G. M.; Whitty, C.; Woo, J. M.; Gallman, A. E.; Miller, T. E.; Levine, A. G.; Nguyen, D. N.; Bapat, S. P.; Balcerek, J.; Bylsma, S. A.; Lyons, A. M.; Li, S.; Wong, A. W.; Gillis-Buck, E. M.; Steinhart, Z. B.; Lee, Y.; Apathy, R.; Lipke, M. J.; Smith, J. A.; Zheng, T.; Boothby, I. C.; Isaza, E.; Chan, J.; Acenas, D. D.; Lee, J.; Macrae, T. A.; Kyaw, T. S.; Wu, D.; Ng, D. L.; Gu, W.; York, V. A.; Eskandarian, H. A.; Callaway, P. C.; Warrier, L.; Moreno, M. E.; Levan, J.; Torres, L.; Farrington, L. A.; Loudermilk, R.; Koshal, K.; Zorn, K. C.; Garcia-Beltran, W. F.; Yang, D.; Astudillo, M. G.; Bernstein, B. E.; Gelfand, J. A.; Ryan, E. T.; Charles, R. C.; Iafrate, A. J.; Lennerz, J. K.; Miller, S.; Chiu, C. Y.; Stramer, S. L.; Wilson, M. R.; Manglik, A.; Ye, C. J.; Krogan, N. J.; Anderson, M. S.; Cyster, J. G.; Ernst, J. D.; Wu, A. H. B.; Lynch, K. L.; Bern, C.; Hsu, P. D.; Marson, A. Test Performance Evaluation of SARS-CoV-2 Serological Assays, *medRxiv*, 2020, DOI: 10.1101/2020.04.25.20074856 (accessed Nov 02, 2021).
(38) Bangdiwala, S. I.; Haedo, A. S.; Natal, M. L.; Villaveces, A. The Agreement Chart as an Alternative to the Receiver-Operating Characteristic Curve for Diagnostic Tests. *Journal of Clinical Epidemiology* **2008**, *61*, 866−874.
(39) Center for Devices and Radiological Health, United States Food and Drug Administration. Self-Monitoring Blood Glucose Test Systems for Over-the-Counter Use: Guidance for Industry and Food and Drug Administration Staff. https://www.fda.gov/regulatory-information/search-fda-guidance-documents/self-monitoring-blood-glucose-test-systems-over-counter-use (accessed April 27, 2022).
(40) Li, L.; Tan, C.; Zeng, J.; Luo, C.; Hu, S.; Peng, Y.; Li, W.; Xie, Z.; Ling, Y.; Zhang, X.; Deng, E.; Xu, H.; Wang, J.; Xie, Y.; Zhou, Y.; Zhang, W.; Guo, Y.; Liu, Z. Analysis of Viral Load in Different Specimen Types and Serum Antibody Levels of COVID-19 Patients. *J. Transl. Med.* **2021**, *19*, 30.
(41) Yang, W.; Zhou, Y.-F.; Dai, H.-P.; Bi, L.-J.; Zhang, Z.-P.; Zhang, X.-H.; Leng, Y.; Zhang, X.-E. Application of Methyl Parathion Hydrolase (MPH) as a Labeling Enzyme. *Anal. Bioanal. Chem.* **2008**, *390*, 2133−2140.
(42) Kobayashi, N.; Iwakami, K.; Kotoshiba, S.; Niwa, T.; Kato, Y.; Mano, N.; Goto, J. Immunoenzymometric Assay for a Small Molecule, 11-Deoxycortisol, with Attomole-Range Sensitivity Employing an ScFv−Enzyme Fusion Protein and Anti-Idiotype Antibodies. *Anal. Chem.* **2006**, *78*, 2244−2253.
(43) Erdag, B.; Balcioglu, K. B.; Bahadir, A. O.; Hinc, D.; Ibrahimoglu, O.; Bahar, A.; Basalp, A.; Yucel, F. Cloning of Anti-HBsAg Single-Chain Variable Fragments from Hybridoma Cells for One-Step ELISA. *Biotechnol. Biotechnol. Equip.* **2017**, *31*, 964−973.
(44) Sasajima, Y.; Iwasaki, R.; Tsumoto, K.; Kumagai, I.; Ihara, M.; Ueda, H. Expression of Antibody Variable Region-Human Alkaline Phosphatase Fusion Proteins in Mammalian Cells. *J. Immunol. Methods* **2010**, *361*, 57−63.
(45) Venisnik, K. M. Bifunctional Antibody-Renilla Luciferase Fusion Protein for in Vivo Optical Detection of Tumors. *Protein Eng., Des. Sel.* **2006**, *19*, 453−460.
(46) Kerschbaumer, R. J.; Hirschl, S.; Schwager, C.; Ibl, M.; Himmler, G. PDAP2: A Vector for Construction of Alkaline Phosphatase Fusion-Proteins. *Immunotechnology* **1996**, *2*, 145−150.
(47) Ritthisan, P.; Ojima-Kato, T.; Damnjanović, J.; Kojima, T.; Nakano, H. SKIK-Zipbody-Alkaline Phosphatase, a Novel Antibody Fusion Protein Expressed in *Escherichia coli* Cytoplasm. *J. Biosci. Bioeng.* **2018**, *126*, 705−709.
(48) Mori, A.; Ojima-Kato, T.; Kojima, T.; Nakano, H. Zipbodyzyme: Development of New Antibody-Enzyme Fusion Proteins. *J. Biosci. Bioeng.* **2018**, *125*, 637−643.
(49) Han, C.; Ihara, M.; Ueda, H. Expression of an Antibody-Enzyme Complex by the L-Chain Fusion Method. *J. Biosci. Bioeng.* **2013**, *116*, 17−21.
(50) Mader, A.; Chromikova, V.; Kunert, R. Recombinant IgM Expression in Mammalian Cells: A Target Protein Challenging Biotechnological Production. *ABB* **2013**, *04*, 38−43.
(51) Chromikova, V.; Mader, A.; Steinfellner, W.; Kunert, R. Evaluating the Bottlenecks of Recombinant IgM Production in Mammalian Cells. *Cytotechnology* **2015**, *67*, 343−356.

https://doi.org/10.1021/jacs.2c02537
J. Am. Chem. Soc. XXXX, XXX, XXX−XXX